Spring 4-5-2015

Measuring the Hyperfine Splittings of Lowest Energy Atomic Transitions in Rubidium

Benjamin D. Graber
Otterbein University, benjamin.graber@otterbein.edu

MEASURING THE HYPERFINE SPLITTINGS OF LOWEST ENERGY ATOMIC TRANSITIONS IN RUBIDIUM

by

Benjamin Daniel Graber
Department of Physics
Otterbein University
Westerville, Ohio 43081

March 17, 2015

Submitted in partial fulfillment of the requirements
For graduation with Honors

_____	_____
Honors Advisor (Please print name)	Advisor's Signature
_____	_____
Second Reader	Second Reader's Signature
_____	_____
Honors Representative	Honors Rep's Signature

Acknowledgments

I would like to thank my research advisor, Dr. Aaron Reinhard, for this tremendous opportunity and for his countless hours of hard work and instruction. Also, a special thanks to Dennis and Barbara Graber; although you don't remember the last time you could help with my math homework, none of this would be possible without your unending love and support.

Abstract

The goal of this experiment was to measure the hyperfine energy splittings of the ground to first excited state transitions in rubidium using saturated absorption spectroscopy. Using this technique, we measured these transition energy spectra by taking the difference of two photodiode outputs due to multiple beams of a single laser scanned over a range of frequencies and shone through a cell of Rb vapor. When the laser frequency was resonant with an atomic transition, photons of those frequencies were absorbed, leaving a dip in intensity of the beam measured at the photodiode. One of the two laser beams had its excitations saturated by a more intense, counter-propagating pump beam from the same laser. The pump beam saturated the absorption of the velocity equal zero atoms that the counter-propagating probe beam could have also interacted with due to no Doppler shift. At these frequencies the probe beam experienced less absorption that was measured by a photodiode. The photodiode output was calibrated to the change in frequency of the scanned laser using a Fabry-Pérot interferometer. The output of this interferometer served as a reference for how the laser frequency changed. Final results for the ^{87}Rb F=1 spectrum accounted for the largest error with a maximum of 12.2% deviation from accepted energy spacing values due in part to systematic error. Other spectra measurements were in better agreement, possessing error ranging from 2.1% to 10.1% and some agreeing with accepted values to within our uncertainty.

Table of Contents

List of Tables

Page

List of Figures

1.0 Introduction

The goal of this experiment was to measure the hyperfine energy splittings of the ground to first excited state transitions in rubidium (Rb) using saturated absorption spectroscopy. Motivations for measuring and understanding these energy spacings include serving as a test of quantum mechanical perturbation theory and also the posterity of research at Otterbein University. Upcoming research will involve laser-cooling rubidium gas and exciting Rydberg states by use of lasers to then study their interactions. A Rydberg state is an energy state of high quantum number n. These Rydberg atoms allow scientists to simulate other condensed matter systems and have applications to areas such as quantum computing and quantum control [1]. The Rydberg states will be excited in stages, the first possibly being from ground to one of the first excited states discussed in this thesis, the energy of which must be precisely known to excite this specific transition.

2.0 Background

2.1 Lasers

The work and experiment in this thesis relied on the use of lasers due to their property of producing coherent light, therefore it is significant to understand how they function. For a perfect coherent beam of light, the photons composing the beam are all the same wavelength, are in phase, and propagate in the same direction.

For many sources of light, such as an LED, electrons typically occupy the lowest energy ground states. Pumping energy into the LED excites electrons into higher, clearly defined, energy states called excited states. From here the electrons can spontaneously

(that is, without external inducement) drop back down energy levels giving off photons with energies corresponding to the energy drop. In this case, photons' direction and phase are random and occur over a range of wavelengths. This case operates via spontaneous emission, however there is another possible mechanism by which the electrons can drop down energy levels, namely stimulated emission. Stimulated emission occurs when the presence of electromagnetic radiation of the proper frequency triggers an electron de-excitation and emission of a photon at the same frequency. This is the condition on which lasers operate. LASER is an acronym for Light Amplification by Stimulated Emission of Radiation. We will consider the fundamentals of stimulated emission in lasers by looking at the first (pulsed ruby) laser (Figure 1) [2].

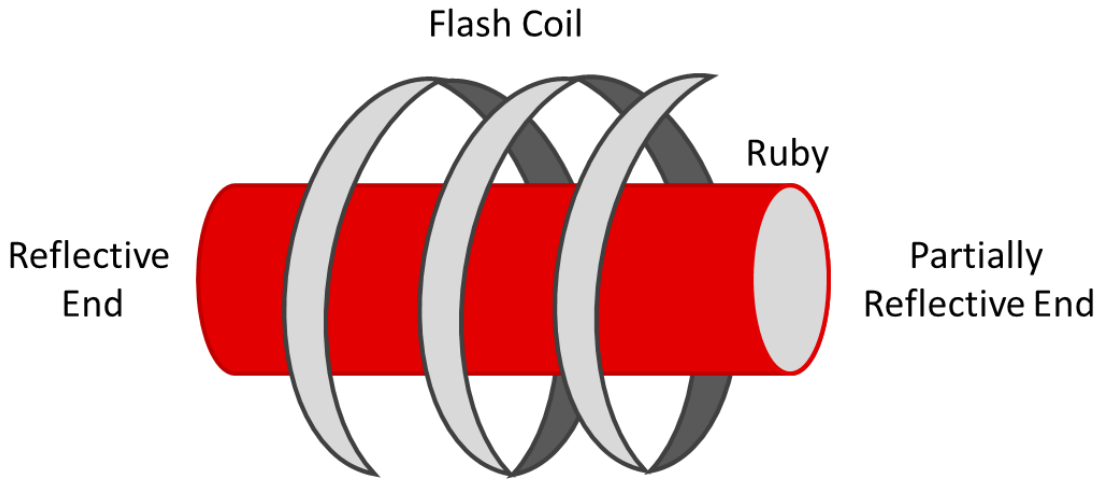

Figure 1: The first (pulsed ruby) laser. A medium of ruby with silvered ends for reflectivity; one completely and the other partially reflective through which some light may exit the medium. A flash coil surrounds the ruby to provide energy to excite atoms in the ruby.

A rod of ruby is silvered on both ends to reflect photons, forming a resonant cavity. One end is partially silvered so that a small fraction of light may exit the ruby on that end. A flash coil surrounds the ruby, providing a broad spectrum of intense light to optically

pump atomic transitions in the ruby. This excites electrons from the ground state to an unstable excited state that, in the case of ruby, quickly decays down to a metastable state through non-radiative transitions, giving off energy to the crystal lattice (Figure 2). The metastable state is named as such due to its particularly long lifetime before decaying. This long lifetime is due to the fact that the energy transition from the metastable state to ground state is quantum mechanically forbidden. In practice the transition still has a probability of occurring but it may take one thousand to one million times longer than the decay time of allowed transitions taking a microsecond or less [3]. For lasers, metastable states are used to maintain population inversions. A population inversion is created in a medium when electrons transition into higher, excited states faster than they naturally decay back to the ground state. By turning up the flash coil high enough in the ruby laser, a population inversion forms and creates a large population of electrons occupying the long-lived metastable state. When an electron drops from the metastable state to the ground state, a photon is emitted with energy equal to the difference of energy states. The frequency of the photon, v, can be solved from the relation in Equation (1) when E_1 and E_0 are energy levels of the metastable state and ground state, respectively, and h is Planck's constant.

$$E_1 - E_0 = hv \tag{1}$$

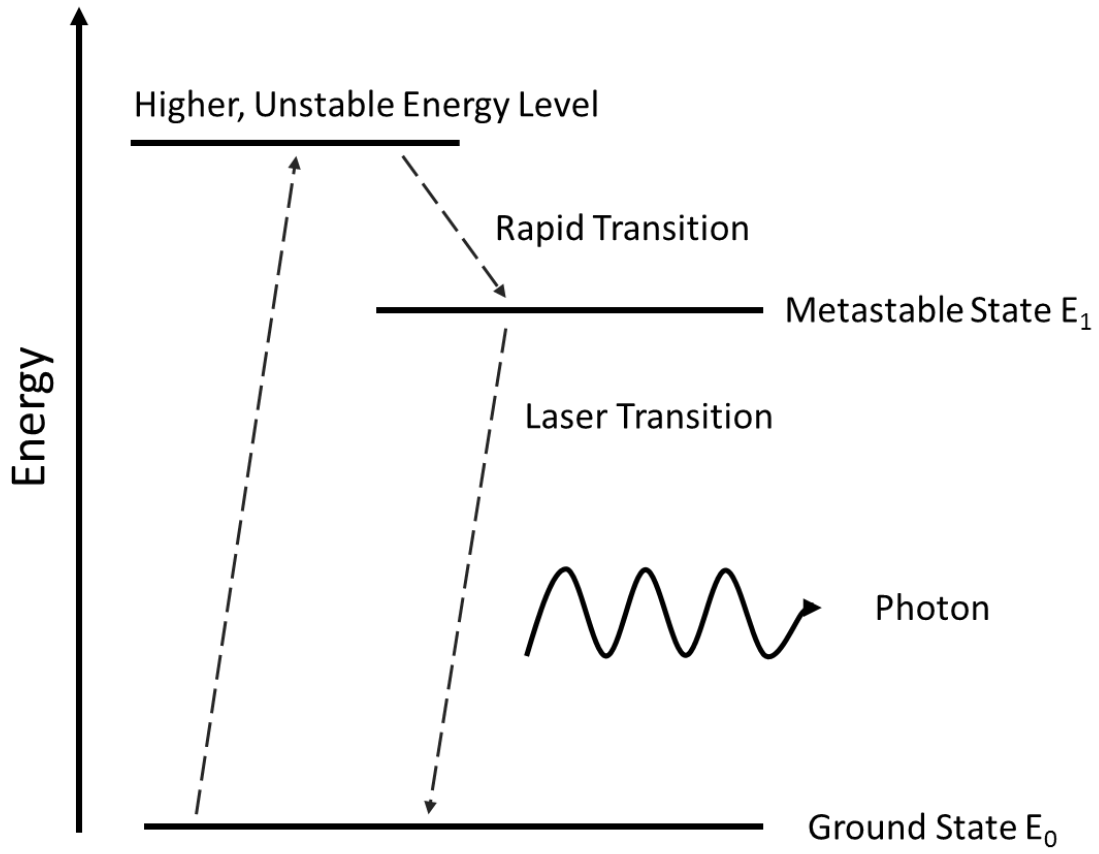

Figure 2: Simplified form of atomic transitions in the first (pulsed) ruby laser. Electrons are pumped by a flash coil into higher energy states and they relax via non-radiative transitions to a metastable state. From here the photons of the transition energy can be released via spontaneous emission, or stimulated emission, when induced by the electric field of an identical photon.

Once one of these photons of frequency ν is emitted, it possesses the electromagnetic field of the appropriate frequency to induce stimulated emission of photons from other electrons populating the metastable state. One photon sets up a chain reaction, inducing stimulated emission of other photons, coherent with the one before it. These photons continue to reflect inside the silvered resonant cavity of the ruby, gaining intensity with the superposition of each additional photon. Some fraction of the photons escape through the partially silvered end becoming the beam of laser light.

2.2 External Cavity Diode Lasers

The laser used in this experiment was an external cavity diode laser (ECDL) [4,5] because they can be used to scan over a range of frequencies of light. Although diodes themselves have a smaller bandwidth than the ruby laser discussed previously, the ECDL setup is used to regulate and narrow this bandwidth; this step is crucial for this experiment because the free-running diode bandwidth is comparable to the scale of the spacings we want to measure. Due to the small reflective cavity of a diode, the light emitted diverges in an oval shape of angles up to 25º. Diodes involve the junction of two semiconductors and operate via properties of solid state physics; it suffices to say that this junction allows free electrons in the solid to occupy the lower energy valence band or higher energy conduction band (Figure 3). Due to the interactions of atoms in the lattice, both of these bands exist over a range of energies. A current through the diode pumps electrons from the valence band up to fill states in the conduction band. When an electron falls back down to the valence band (via spontaneous or stimulated emission), a photon is emitted with an energy corresponding to the energy difference. Since electrons could occupy a range of different energies within both bands, there is a nonzero bandwidth of the corresponding light emitted.

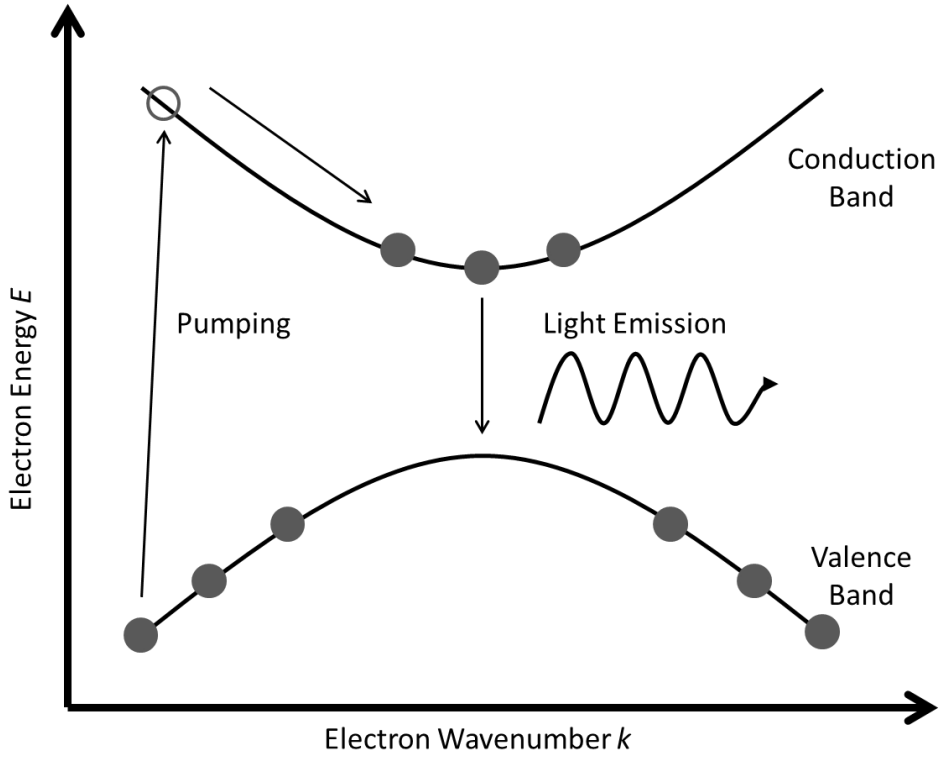

Figure 3: Free electrons at the semiconductor junction of diodes can occupy a range of energies in the valence band or the excited conduction band. Current across the diode pumps electrons up into the conduction band, where they drop back down to the valence band via spontaneous or stimulated emission, giving off light of energy equal to the energy difference.

The diode outputs a diverging, oval-shaped beam, making it impractical for many experimental purposes; however the beam can be aligned for minimal beam divergence using a lens (or lenses). The focal point of a lens is the point at which all light parallel to the normal axis of the lens converges (Figure 4). By placing our diode at the focal point, outgoing light converges to a nearly parallel beam. Also, any incoming light travelling antiparallel to this beam is focused directly back to the diode at the focal point of the lens. This property allows for the use of optical feedback to the diode.

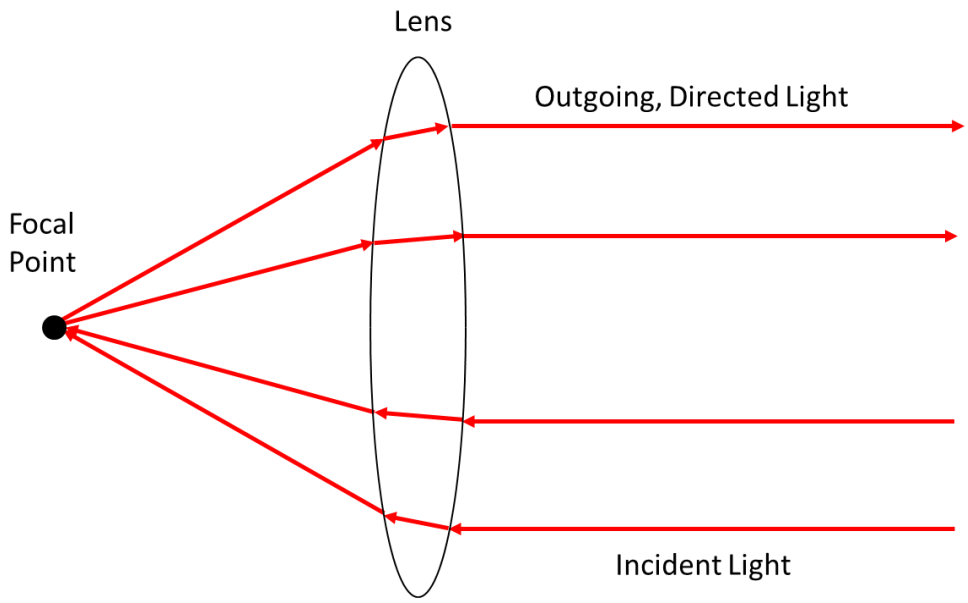

Figure 4: The focal point of a lens is the point at which all light parallel to the normal axis of the lens is focused. Also, light emitted from the focal point is bent parallel to the normal axis of the lens.

Optical feedback is used on the diode in an ECDL to narrow the bandwidth of its output to a narrow range of frequencies. This is accomplished using a blazed diffraction grating; an asymmetric optical component with finely scored, periodic ridges, whose geometry diffracts specific orders of light. This special type of diffraction grating is used to optimize efficiency along a given diffracted order. For a system aligned in the Littrow configuration, the diffracted beam is sent directly back along the direction of the incident beam. Resulting diffractions from a blazed diffraction grating in a Littrow configuration are given by the Bragg condition in Equation 2. For a complete explanation of blazed diffraction gratings we refer to Palmer's *Diffraction Grating Handbook* [6].

$$2d \sin\theta = n\lambda \qquad (2)$$

Here, d is the line spacing of the diffraction grating, n is an integer, λ is the wavelength of incident light, and θ is the angle of incidence. For a given wavelength of light, this

condition gives the angles of constructively interfering light. The reflected beam off the blazed grating is the most intense and will be used as the beam sent from the laser to the rest of the experiment. A percentage of the incoming light is diffracted according to Equation 2 and in our Littrow configuration the $n = -1$ order shines straight back into the laser. This order is the optical feedback that drives and regulates the laser's output. The optical feedback beam of a specific wavelength propagates back into the diode, where it induces the stimulated emission of an identical photon, driving the laser at this wavelength of light. This results in a laser output with this specific, narrow bandwidth of light, significantly smaller than the diode's full bandwidth ($20MHz \rightarrow 2MHz$). Now consider slightly changing the angle of the diffraction grating, thus slightly changing θ. Now if θ is changed, the light going back into the diode (which satisfies the Bragg condition in Equation 2) has a different wavelength, λ. This is the new wavelength that diffracts back to the laser as optical feedback, thus driving stimulated emission of identical photons to be emitted. By scanning the diffraction grating over a range of angles, the ECDL emits a narrow bandwidth of light over a scanned range of wavelengths. The bandwidth of this narrower range is limited by the physical width of the diode allowing a range of frequencies to be reflected back into the diode.

2.3 Doppler Effect

To understand saturated absorption spectroscopy, we must first understand the Doppler effect, because this effect serves as both the cause for the need of the technique as well as the solution. The Doppler effect is the change in frequency of a wave due to relative velocity between the wave source and an observer. Consider a wave source that has a velocity of zero relative to its observers and emits wave fronts radially out in all

directions (Figure 5). The circles represent the same reference point on the produced wave, each one period apart; the innermost circle corresponds to the most recent wave crest, preceded by the previous circles outside that have had more time to travel. The wave fronts reach both observers at the same frequency that they were emitted by the source. The observers do not experience a Doppler shift in frequency of the wave.

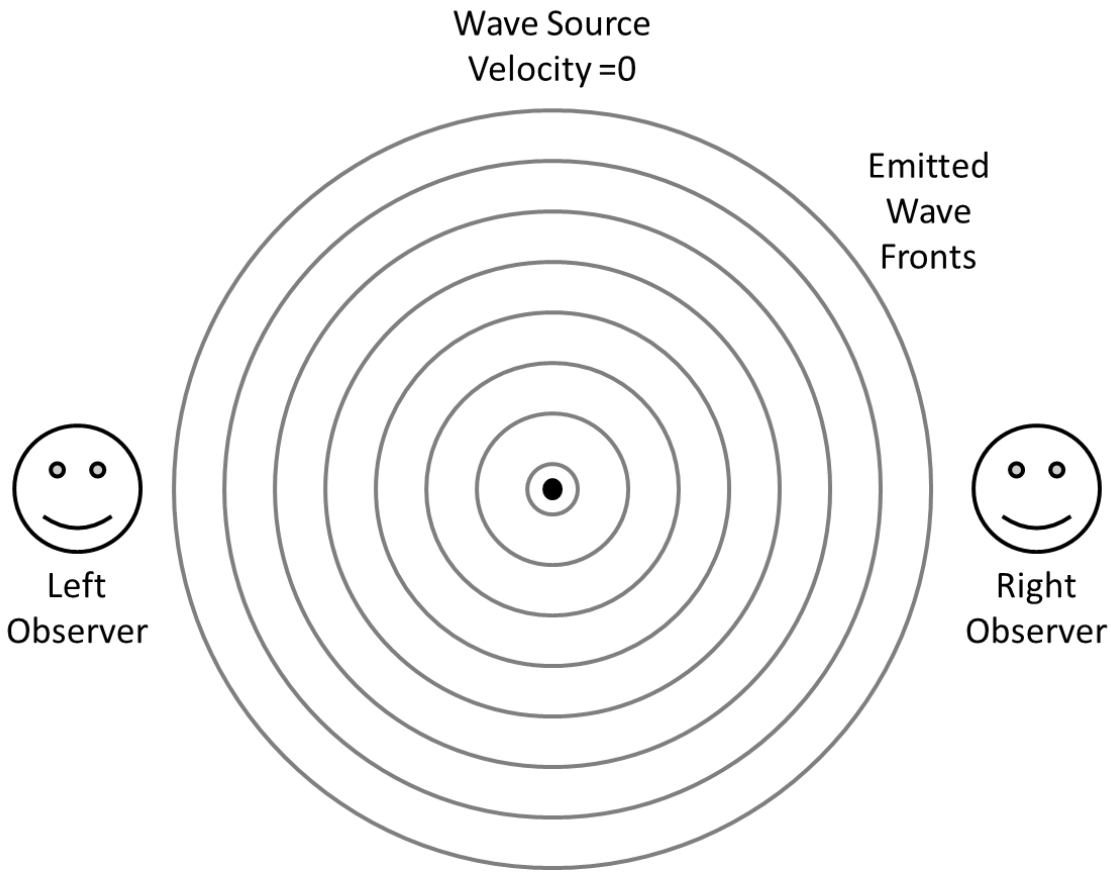

Figure 5: Center wave source has a velocity of zero relative to both observers. Both observers detect the same wave frequency as was emitted by the source.

Now consider the wave source moving to the right with some velocity but still emitting waves with the same frequency as before (Figure 6). The relative velocity of the source toward the right observer causes the right observer to perceive more wave fronts in the same amount of time, thus Doppler shifting to a higher frequency. Similarly, the

relative velocity of the source away from the left observer causes the left observer to perceive fewer wave fronts in the same amount of time, Doppler shifting to a lower frequency. This will be important in saturated absorption spectroscopy because the frequency of light absorbed by an atom depends on their relative velocity.

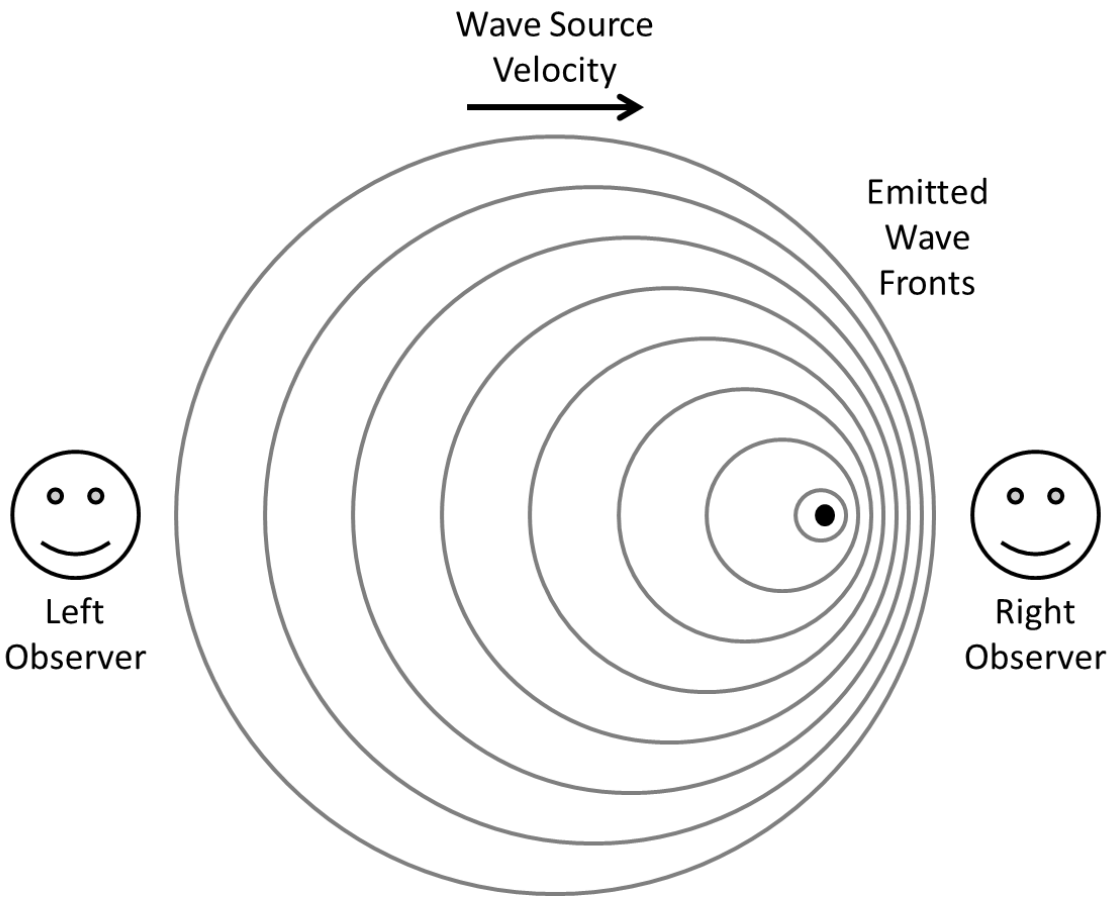

Figure 6: Center wave source travels with a velocity to the right relative to the observers. The right observer perceives a higher frequency, and the left observer perceives a lower frequency than the source frequency via Doppler Effect.

3.0 Methods

The spectrum of lowest energy atomic transitions in rubidium was measured using saturated absorption spectroscopy. This technique involved shining a laser beam through a cell of room-temperature rubidium vapor and cycling the laser over a small

range of frequencies $\Delta f \approx 1.5GHz$ also known as the free spectral range. To do this, I constructed an external cavity diode laser (ECDL) using raw materials and modifying manufactured parts (this ECDL can be seen in appendices A1). For this experiment the laser was tuned to an infrared wavelength around the ground to first excited state energy of Rb, $\lambda \approx 780.245nm$ and the grating used was a blazed, gold, holographic diffraction grating with 1,800 $\frac{lines}{mm}$. The ECDL (Figure 7) was scanned over a small range of frequencies, according to the Bragg condition (Equation 2), using a piezoelectric transducer (PZT). A PZT is a device that changed its length proportionally to its applied voltage. Driving the PZT's voltage with a triangular wave from a function generator scanned the angle of the diffraction grating, thus cycling the wavelength, λ, of the laser.

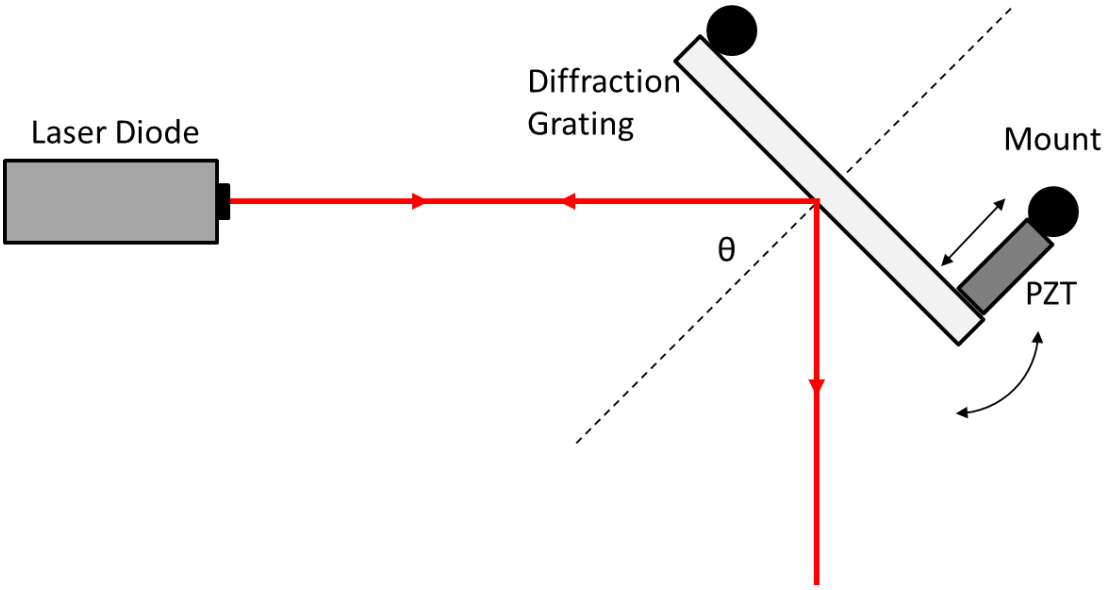

Figure 7: External Cavity Diode Laser (ECDL) operates via the use of a diffraction grating; The PZT changes length proportional to applied voltage, changing the wavelength of the refracted order that is directed back to the laser as optical feedback. This feedback drove the frequency of the output of the laser.

An oscilloscope recorded the scanned voltage output from the function generator as a function of time but this did not tell how the frequency of the laser output was changing.

To find this we used interferometers, or optical devices used to make measurements of changes in laser frequency using the principle of superposition (Figure 8). By the interferometer geometry, we solved the frequency change of our laser as a function of applied voltage, thus calibrating the oscilloscope time units into a frequency change of the laser. This experiment utilized both a Michelson and a Fabry-Pérot Interferometer to measure the change in frequency of the laser output and therefore the change in frequency of rubidium's energy splittings excited by this laser.

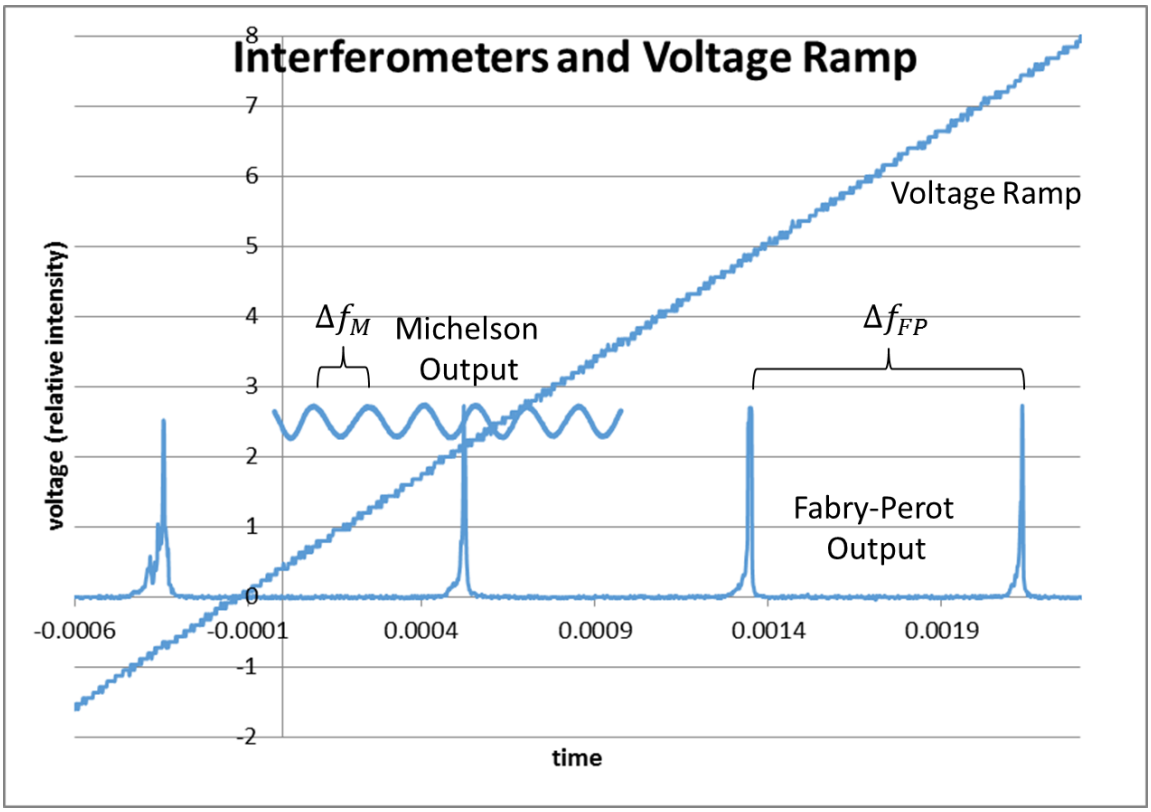

Figure 8: As the voltage ramp changed the frequency of the laser, the interferometers produced periodic outputs when Δf between successive peaks resulted from the geometry of the interferometer.

3.1 Michelson Interferometer

The Michelson interferometer (Figure 9), used a 50:50 beamsplitter to split an incident laser into two separate beams, each travelling different lengths before

recombining and shining on a photodiode. The photodiode output a voltage to an oscilloscope that was proportional to the intensity of light shone on it. Intensity (I) of light is given by

$$I = \left|\vec{E}\right|^2 = \vec{E} \cdot \vec{E}^* \quad (3)$$

where $\vec{E}^*$ is the complex conjugate of $\vec{E}$, the electric field of the light (Equation 4).

$$\vec{E}(x) = \vec{E}_0 e^{i(kx-\omega t)} \quad (4)$$

The electric field at the photodiode resulted from the combination of the two beams, which travelled different lengths and therefore have different phases depending on wavelength of the light. Total electric field at the photodiode from both beams was

$$\vec{E}_{total} = \vec{E}(L) + \vec{E}(L + \Delta L) \quad (5)$$

Using Equations 3 and 4 for $\vec{E}_{total}$, and the distances $x = 2(L)$ and $x = 2(L + \Delta L)$, because the beams travelled both down and back, the intensity was solved to be

$$I = 2E_0^2[1 + \cos(2k\Delta L)] \quad (6)$$

This demonstrates that intensity was periodic in the quantity $2k\Delta L$, meaning that if this value changed by an integer of 2π, intensity returned to the same value. Wavenumber, k, changed as the frequency of the laser scanned because

$$k = \frac{2\pi}{\lambda} = \frac{2\pi f}{c} \quad (7)$$

In order to calibrate the frequency from this periodic output, we considered the change in frequency between peaks of the oscillation, Δf_M (Figure 8). Over this period the change

in the periodic quantity $2k\Delta L$ was 2π, such that intensity returned to the same peak value (Equation 8).

$$\Delta(2k\Delta L) = 2\pi \tag{8}$$

Here, ΔL was a constant from the geometric setup of the interferometer, but k changed as the frequency of the laser was scanned, yielding, from Equation 7,

$$\Delta k = \frac{2\pi\Delta f}{c} \tag{9}$$

Plugging this relation into Equation 8, we evaluated for Δf_M (Equation 10).

$$\Delta f_M = \frac{c}{2\Delta L} \tag{10}$$

Therefore, using ΔL, a property of the Michelson interferometer setup, we solved for the frequency between Michelson peaks, Δf_M. Dividing this change in frequency by the period T, or time between peaks, yielded the change in frequency per unit time t for our voltage ramp parameters (Equation 11).

$$\frac{\Delta f_M}{T} = \frac{\Delta f}{t} \tag{11}$$

It followed that our calibration factor was found to be

$$\frac{\Delta f_M}{t} = 507 \cdot 10^9 \pm 4 \cdot 10^9 \ \frac{1}{s^2} \tag{12}$$

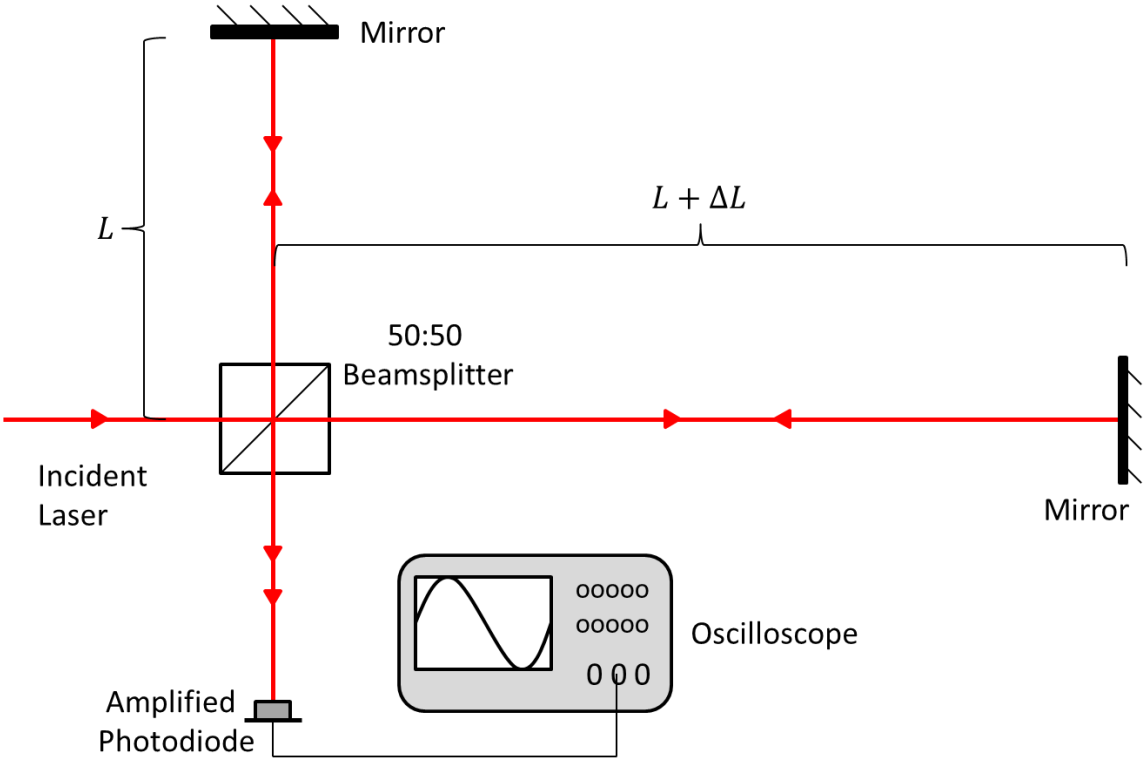

Figure 9: Michelson Interferometer setup. Incident light split at a 50:50 beamsplitter where it traveled 2 different length paths before recombining on a photodiode at different phases, depending on the wavelength.

3.2 Fabry-Pérot Interferometer

The second interferometer used to calibrate the laser drive voltage to frequency was a Fabry-Pérot Interferometer (Figure 10). For this interferometer, two spherically curved, 99% reflective mirrors were separated by the twice their radius of curvature. With the two highly reflective mirrors facing inward, only a small fraction of light could enter or exit the cavity and light continued to reflect inside, like in a resonant cavity. In this "confocal" setup, any incident laser light was reflected back to its point of incidence after four passes through the cavity, as seen by the bowtie-shaped path in Figure 10. Only certain wavelengths of light travelled the bowtie-shaped path of length 4L arriving back

in phase with its incident wave. This occurred when the distance travelled was equal to an integer multiple of the wavelength (Equation 13).

$$4L = n\lambda \tag{13}$$

According to the principle of superposition, these waves were in phase with one another, constructively interfered and increased in intensity with each additional pass. Converting the wavelength of light to frequency using Equation 14, the frequencies that satisfied this constructive condition were solved (Equation 15).

$$c = f\lambda \tag{14}$$

$$f = n\frac{c}{4L} \tag{15}$$

For wavelengths that did not satisfy this condition, each pass through the cavity arrived out of phase with the pass before it, thus destructively interfering with the wave over several passes. The scanned laser light was shone through the interferometer and onto a photodiode to measure its intensity and plotted as a function of time by an oscilloscope (Figure 8). Only the select frequencies of light resonated in the cavity and built up such a strong intensity that an appreciable fraction of light passed through the interferometer mirror to the photodiode. These frequencies corresponded to the narrow voltage peaks of Figure 8. Each successive peak was the next integer n that satisfied the condition on Equation 15, so the frequency change between any two consecutive peaks (Δf), call them peaks n and $n + 1$, was given by Equation 16.

$$\Delta f = \frac{c}{4L} \tag{16}$$

As with the Michelson Interferometer, we solved for the frequency between peaks, Δf_{FP} using L, a property of the interferometer setup. Dividing this change in frequency by the period T, or time between peaks, yielded the change in frequency per unit time t (Equation 17).

$$\frac{\Delta f_{FP}}{T} = \frac{\Delta f}{t} \tag{17}$$

This calibration factor was found to be

$$\frac{\Delta f_{FP}}{t} = 454 \cdot 10^9 \pm 2 \cdot 10^9 \ \frac{1}{s^2} \tag{18}$$

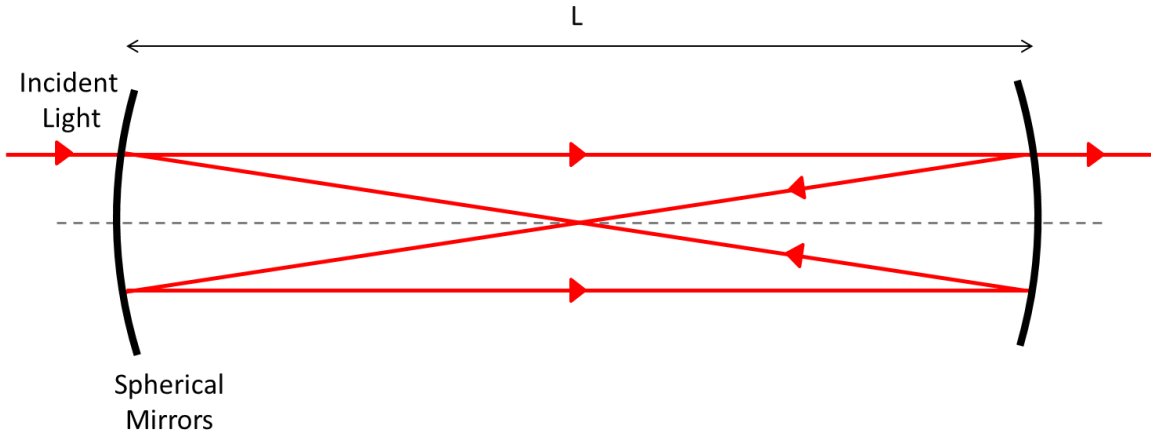

Figure 10: The Fabry-Pérot Interferometer operated on the principle that light reflected in the cavity back to its origin and that only specific wavelengths of light recombined constructively. Over many passes, these wavelengths were intense enough for an appreciable number of photons to escape through the highly reflective mirrors while others were not.

3.3 Saturated Absorption Spectroscopy

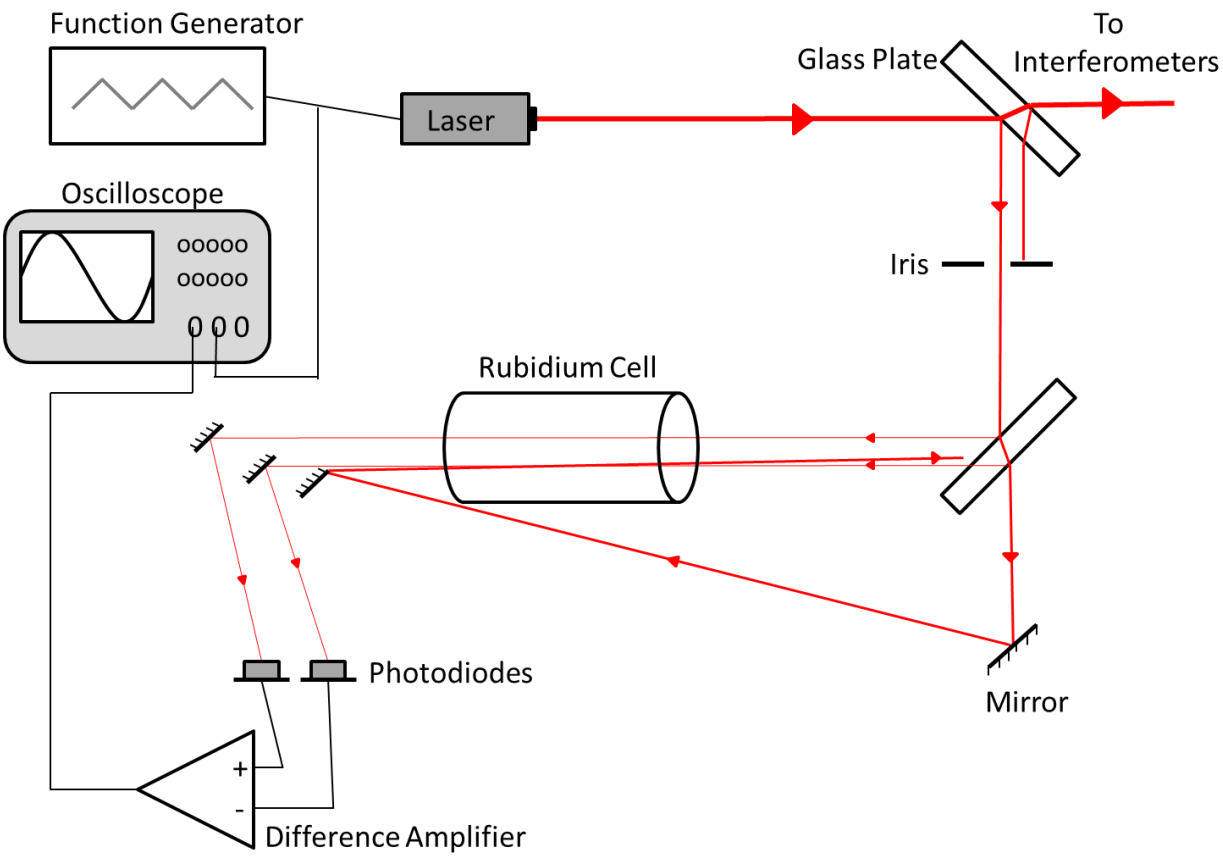

Figure 11: Schematic of apparatus for saturated absorption spectroscopy. Two strands of probe beam from ECDL passed through a Rb cell to photodiodes, whose difference was plotted on an oscilloscope. One probe beam shone antiparallel to a more intense pump beam.

The energy splittings of the $5S_{1/2} \rightarrow 5P_{3/2}$ transition in rubidium were measured using saturated absorption spectroscopy; the setup for this technique is seen in Figure 11. In saturated absorption spectroscopy, the ECDL was scanned over a small range of frequencies and the beam was shone through a glass plate before heading to the interferometers. The glass medium however had a small reflectivity which reflected a small portion of the beam at the front and back faces of the glass. One of these beams

was shone through another glass plate where the two reflected, less-intense "probe beams" were passed through a cell of rubidium vapor and shone onto photodiodes.

As the laser frequency was scanned, the photodiodes measured dips in the intensity of laser light at certain frequencies corresponding to absorption of the probe beam's photons that excited atomic transitions in Rb. The absorption of probe beam photons, as a function of frequency, formed a Gaussian; absorption occurred over a range of frequencies, centered and peaked about the resonant frequency f_0 of an energy transition (Figure 12). The width of this Gaussian is called the "Doppler width" and is much greater than the natural linewidth of a transition. This range of absorption occurred due to the Doppler Effect and Rb cell atoms with non-zero velocity. For a left-travelling probe beam at frequency f_0, $v = 0$ atoms would absorb photons. However absorption also occurred for other frequencies near f_0. For a right-moving atom and a slightly lower frequency $f < f_0$, the frequency seen by the atom in its moving frame would be Doppler shifted up into resonance and absorbed. Inversely, for a left-moving atom and a slightly higher frequency $f > f_0$, the frequency seen by the atom in its moving frame would be Doppler shifted down into resonance and absorbed.

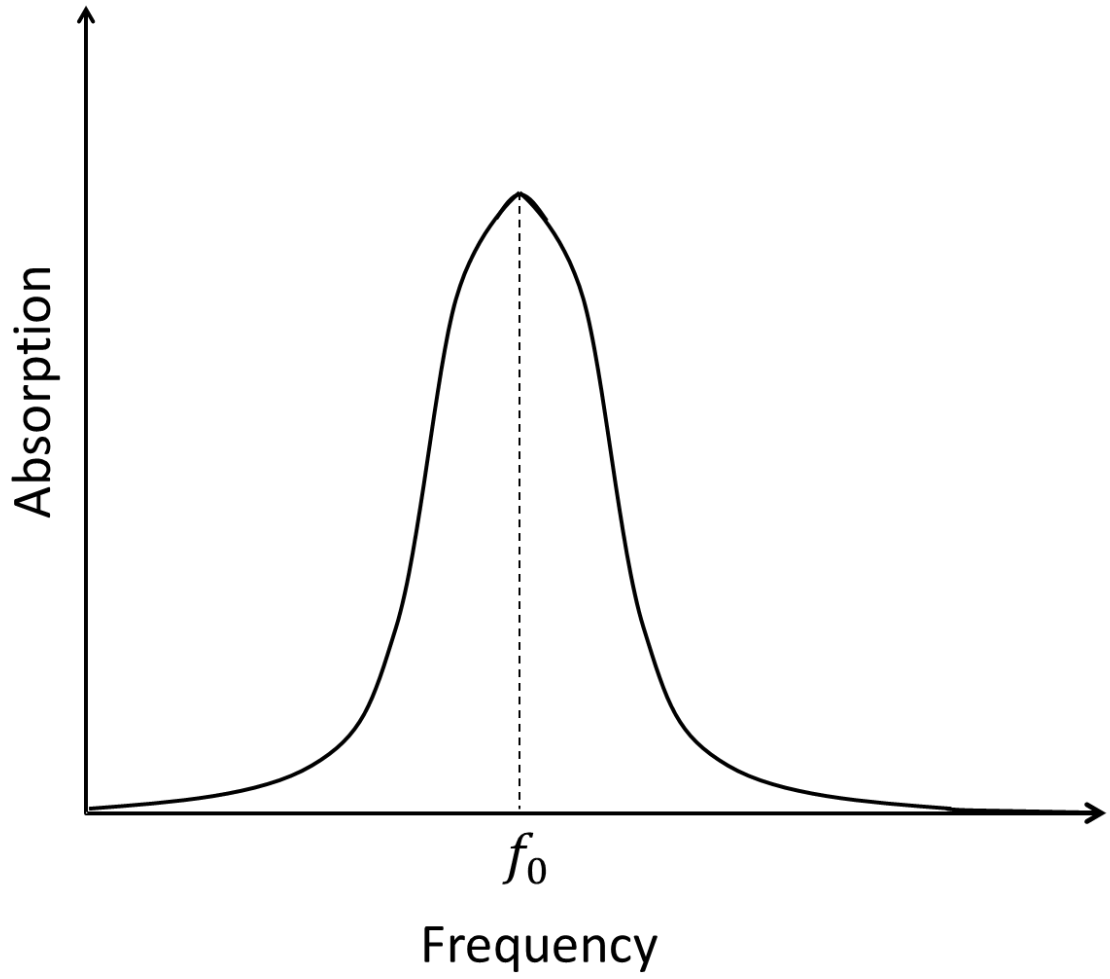

Figure 12: Absorption profile of the probe beam centered about the resonant frequency f_0 of an excitation. Absorption occurred for a range of frequencies around f_0 due to Doppler shift of the laser seen by room temperature Rb atoms of non-zero velocity.

The two "probe beams" were the less intense reflections off the faces of the glass plate but most of the intensity of the beam passed through the glass. This more intense "pump beam" was redirected using mirrors such that it overlapped and propagated antiparallel to one of the two probe beams (Figure 13). This intense beam excited a significant number of atoms on energy transitions that were resonant with or Doppler shifted into resonance with the beam's frequency, thus saturating these transitions.

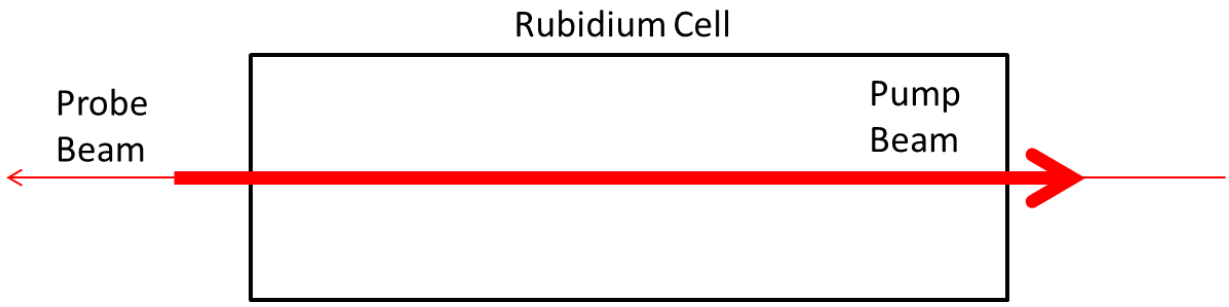

Figure 13: The Probe beam and more intense Pump beam overlapped and propagated in opposite directions through the Rb cell. The Pump beam saturated absorptions of transitions resonant with or Doppler shifted into resonance with its frequency.

Both pump and probe beams derived from the same laser, therefore were the same frequency and for frequencies not equal to f_0, they did not excite the same velocity group of atoms. For the right-moving atom that was absorbed by the probe beam of frequency $f < f_0$ by being upshifted into resonance, the pump beam would not interact with this atom at all. The Doppler Effect downshifted the frequency even further from resonance with the right-travelling pump beam. Only at f_0 did both probe and pump beams interact with the same atoms, those with $v = 0$ so as to not be Doppler shifted out of resonance with either beam. The pump beam was much more intense and saturated all of these excitations, leaving a sharp dip of absorption of the probe beam at f_0, called a Lamb dip (Figure 14). These lamb dips have a much narrower frequency width and better resolution than the Doppler width because they come from $v = 0$ atoms; the Doppler width was so wide that the Gaussian for each hyperfine splitting overlapped and obscured results. Lamb dips are much narrower and of the scale of the natural line width ($6 \pm 0.0018\ MHz$ for the $5S_{1/2} \rightarrow 5P_{3/2}$ transition [7]) plus a small width due to inhomogeneous broadening from collision broadening.

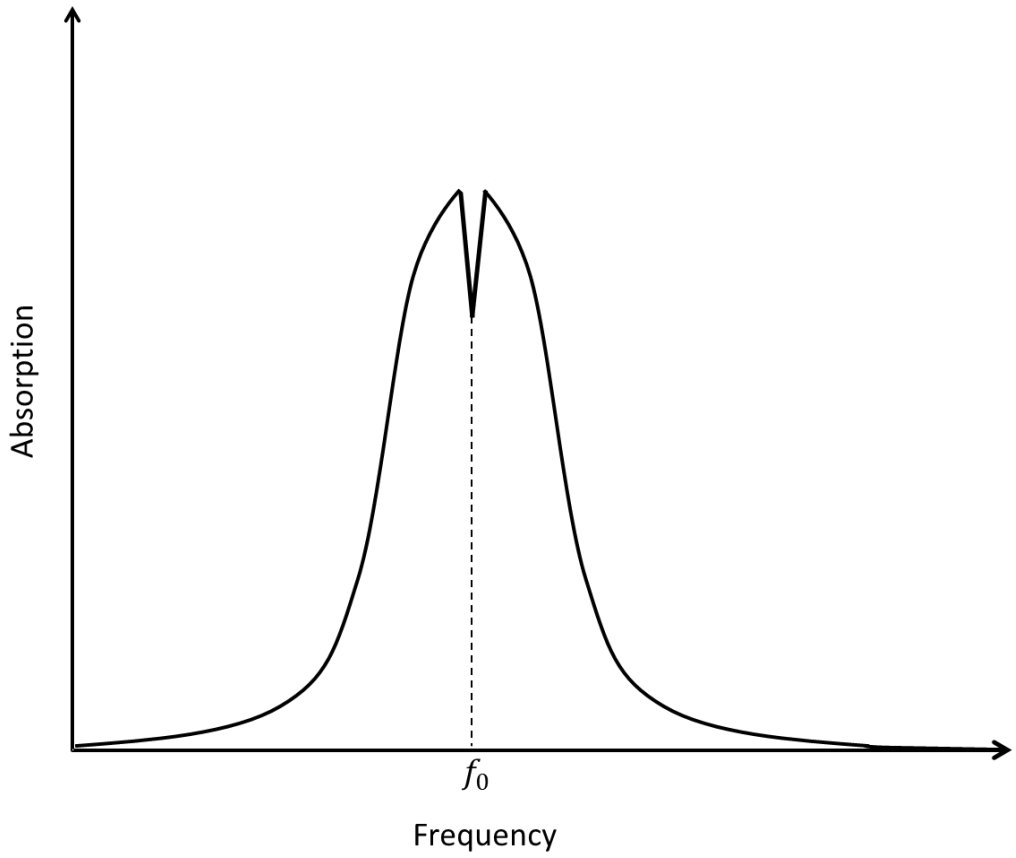

Figure 14: Saturated Absorption profile of the probe beam with a Lamb dip at resonant frequency f_0 due to saturation of these transitions by the pump beam.

The only difference in absorption between the base probe beam and the probe beam saturated by the pump beam (Figures 12 and 14 respectively) was the Lamb dip, so the difference between these outputs left just the defined dips at the resonant frequencies. A difference amplifier took the difference of the photodiode's outputs and I plotted the difference on an oscilloscope. Figure 15 shows this output for the case of the $5P_{3/2}$ hyperfine energy states excited from the ^{87}Rb $5S_{1/2}$ F=2 ground state plotted alongside the voltage ramp to the ECDL and interferometer data.

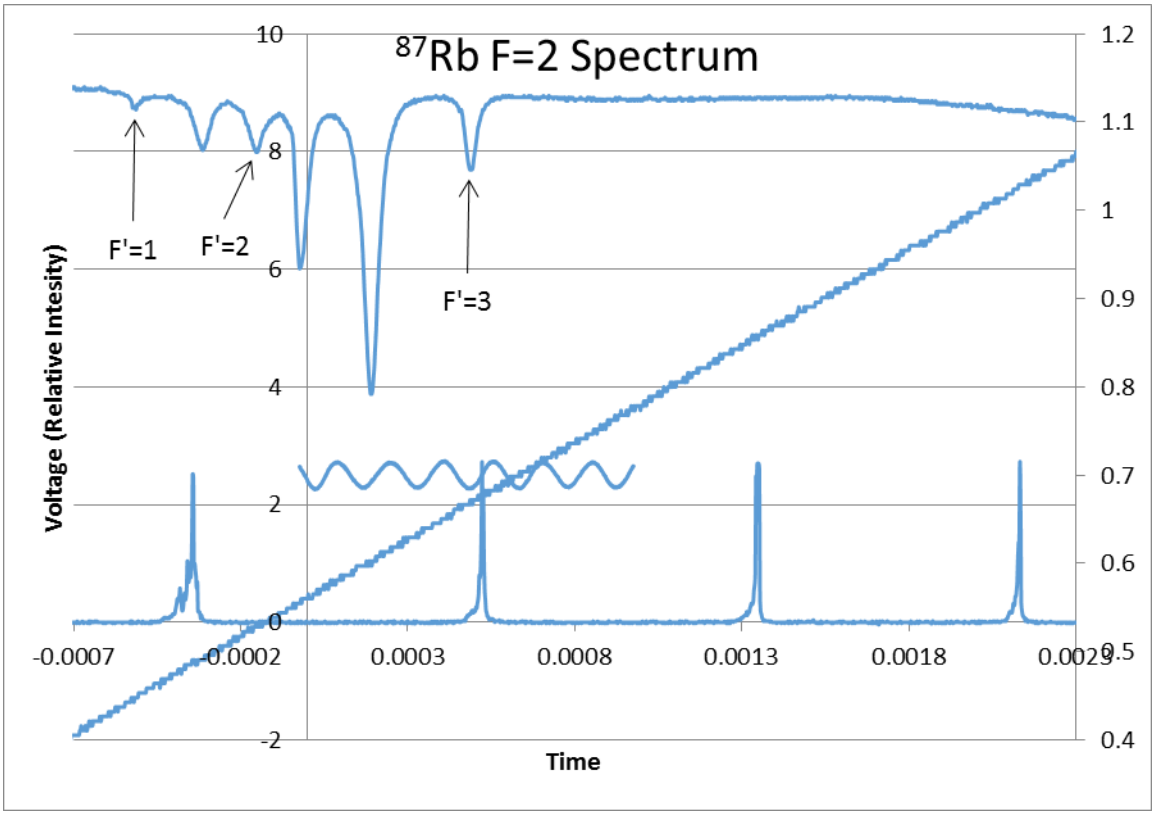

Figure 15: Hyperfine energy splittings of the ^{87}Rb F=2 ground state to first excited state transitions. Plot also includes voltage ramp to ECDL, Michelson and Fabry-Pérot Interferometer output.

In the rubidium cell were the two naturally occurring isotopes, ^{85}Rb and ^{87}Rb (natural abundances of 72% and 28% respectively), each with unique energy levels; their ground and first excited state energy levels are shown in Figure 16. For rubidium's single electron in the outer $5S_{1/2}$ shell, there are two F states in which it could exist. The electron is only quantum mechanically allowed to transition to another state with F that is equal to or different by ± 1 from its own value of F. So an electron in the ^{87}Rb $5S_{1/2}$ F=2 state is only allowed to transition to states with $F = 1,2,3$. However, Figure 15 exhibited six dips, which is more than the three expected lamb dips due to allowed transitions from the ^{87}Rb F=2 state. These extra peaks are known as "crossover peaks."

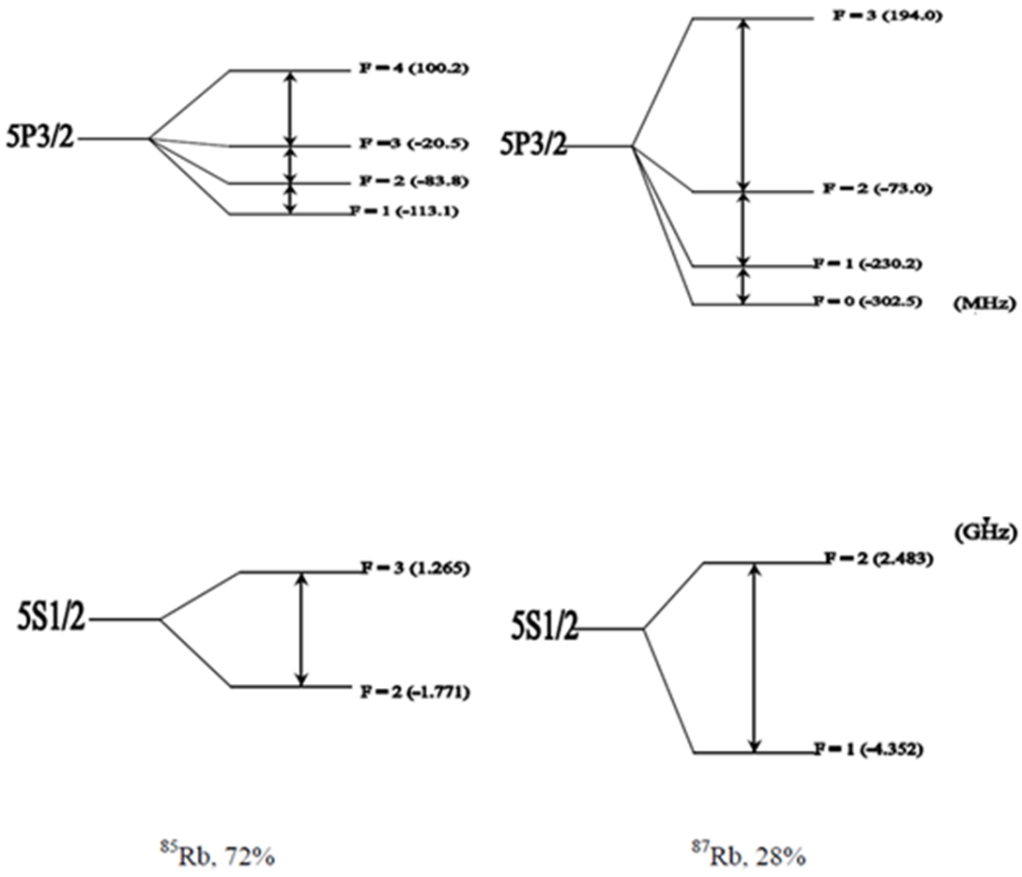

Figure 16: Ground and first excited state hyperfine energy splittings for rubidium's naturally occurring isotopes, ^{85}Rb and ^{87}Rb.

3.4 Crossover Peaks

Figure 15 contained six peaks, which is greater than the three peaks that corresponded to the quantum mechanically allowed transitions. These extra peaks, or "crossover peaks," are an artifact of the saturated absorption technique applied to atoms having multiple allowed energy transitions from a common initial state, in this case the various hyperfine energy states excited from the common $5S_{1/2}$ ground state. This scenario can be seen in Figure 17 where the ground state energy is E_g and the energies of two allowed excited state splittings are E_1 and E_2. Frequencies corresponding to these transitions are f_1 and f_2 respectively.

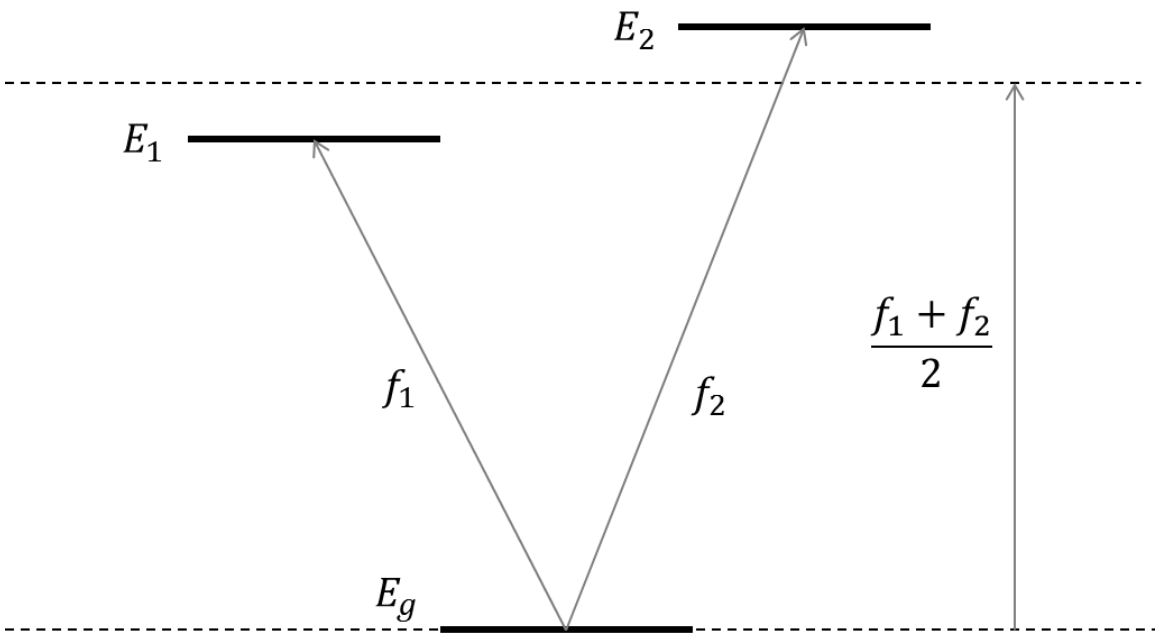

Figure 17: Saturated absorption produced crossover peaks in the spectra halfway between E_1 and E_2 when these transitions shared a common initial state, E_g

If we consider the laser at an excitation frequency halfway in-between the energy splittings $\frac{f_1+f_2}{2}$ and again follow convention of Figure 13, an atom with a certain velocity to the right could be Doppler shifted up into resonance with the probe beam to E_2 and also downshifted into resonance with the pump beam to E_1. Both beams interact with these same velocity atoms but the pump beam excites atoms of a given velocity from the ground state so the probe beam registers a dip in absorption for the same atoms. This dip is a crossover peak and occurs exactly halfway in-between the two real energy transitions. The measured dips resulted from the saturated absorption technique and were disregarded from actual physical meaning in the atom. However, these dips can be used to determine which dips correspond to real energy transitions and as a check for the hyperfine splitting measurements.

4.0 Results

Using saturated absorption spectroscopy, the hyperfine energy spacings of the first excited state in rubidium were measured. Peak maxima were located by fitting parabolas to their data points recorded by the oscilloscope and using the fit equation to solve for their vertices. In the case of non-parabolic peaks, peak location was determined visually. For both cases, an uncertainty of peak location was also recorded.

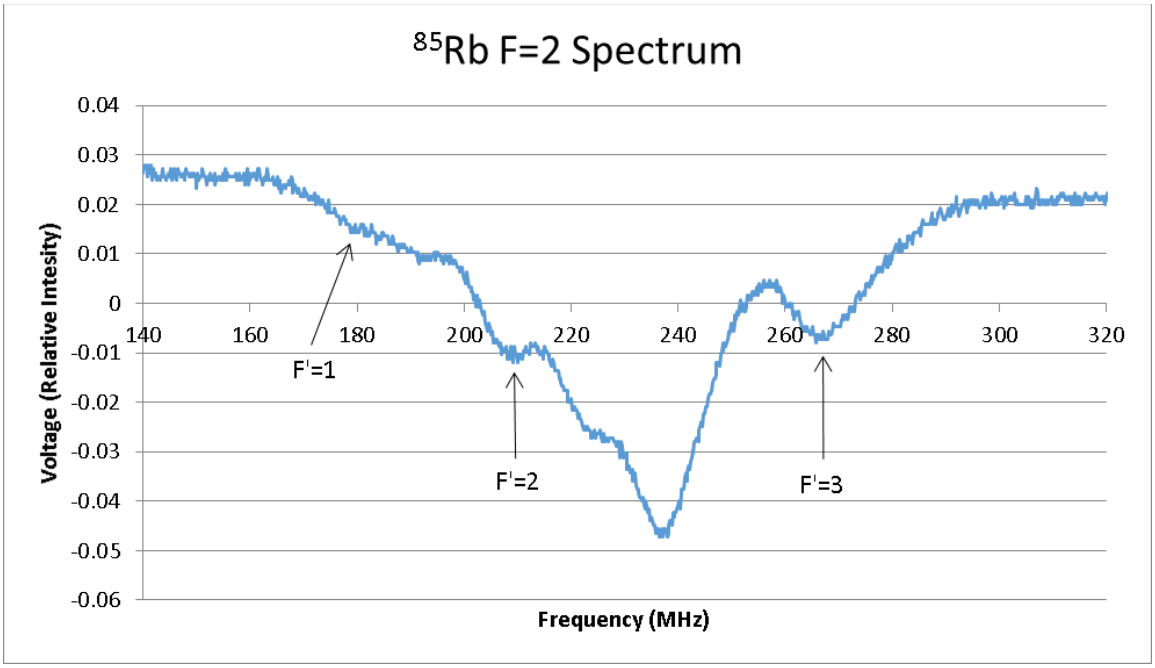

Figure 18: Spectrum of hyperfine energy splittings from the ^{85}Rb F=2 ground state to first excited state transitions.

85Rb F=2 Spectrum		
Frequency Spacing (MHz)		**Accepted Values**
F'=1 & 2	30 ± 8MHz	29.372 ± 0.090MHz
F'=2 & 3	57 ± 4MHz	63.401 ± 0.061MHz
F'=1 & 3	87 ± 8MHz	92.773 ± 0.109MHz

Table 1: Measured and accepted energy spacings between the ^{85}Rb F=2 ground state to first excited state transitions. Accepted values [8,9]

For the ^{85}Rb F=2 spectrum, the energy splittings are naturally small enough that the resulting absorption spectrum Lamb dips are all close together and overlap one another; this causes peaks to be less defined and also shifts the peaks due to the superposition of peaks with sloped side of adjacent Lamb dips. Due to these factors, there is a larger uncertainty associated with locating the peaks, and therefore the energy splittings. Final results could have been improved using more advanced data analysis programs that accounted for the superposition of each Lamb dip. Such programs could fit 6 unconstrained peaks to the spectrum under the condition that three of the peaks had a peak located precisely half-way between them. This method would accurately locate each of these peaks, taking into account all the superposition on the spectrum.

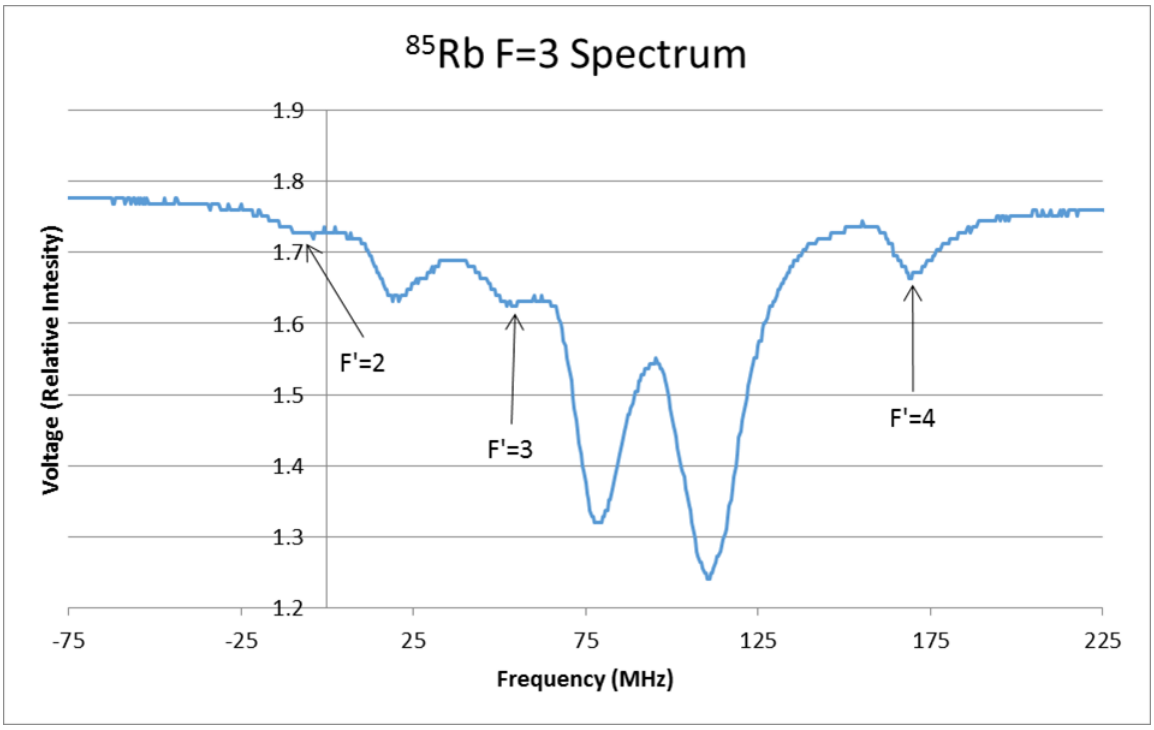

Figure 19: Spectrum of hyperfine energy splittings from the ^{85}Rb F=3 ground state to first excited state transitions.

85Rb F=3 Spectrum		
Frequency Spacing (MHz)		**Accepted Values**
F'=2 & 3	64 ± 10MHz	63.401 ± 0.061MHz
F'=3 & 4	116 ± 5MHz	120.640 ± 0.068MHz
F'=2 & 4	179 ± 10MHz	184.041 ± 0.091MHz

Table 2: Measured and accepted energy spacings between the ^{85}Rb F=3 ground state to first excited state transitions. Accepted values [8,9]

The ^{85}Rb F=3 spectrum peaks are further spaced and cleaner than the previously mentioned ^{85}Rb F=2 spectrum. Final measurements were within a smaller uncertainty and agreed with the current accepted values.

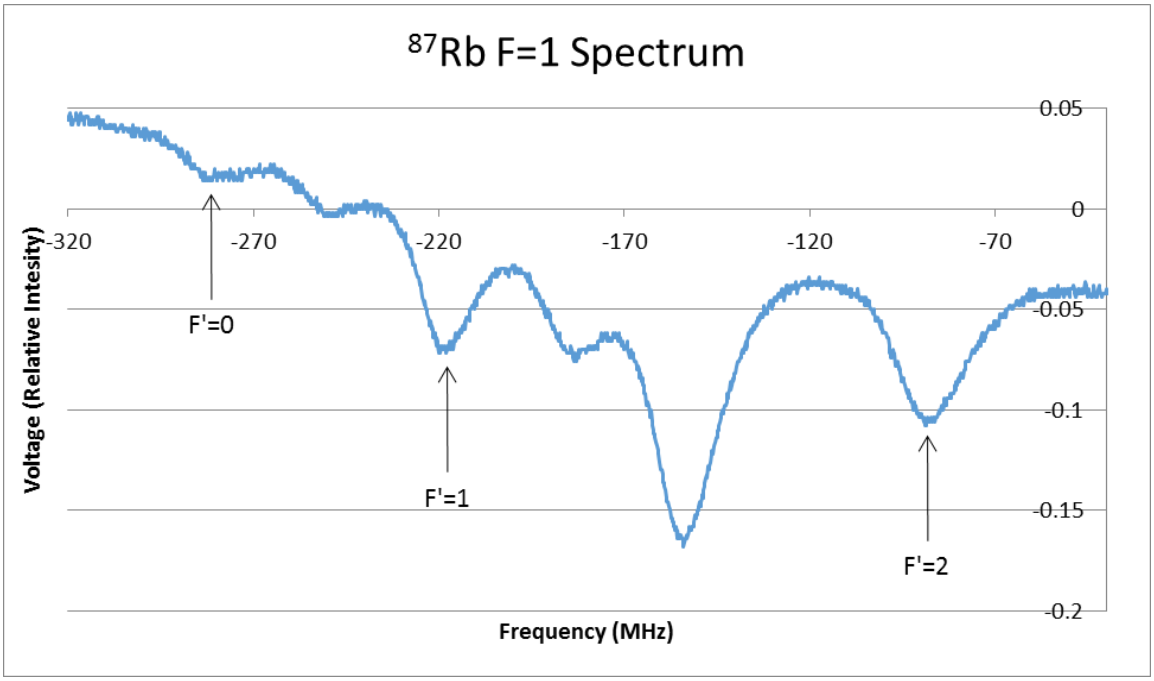

Figure 20: Spectrum of hyperfine energy splittings from the ^{87}Rb F=1 ground state to first excited state transitions.

87Rb F=1 Spectrum		
Frequency Spacing (MHz)		**Accepted Value**
F'=0 & 1	81 ± 7MHz	72.218 ± 0.004MHz
F'=1 & 2	164 ± 4MHz	156.947 ± 0.007MHz
F'=0 & 2	245 ± 7MHz	229.165 ± 0.008MHz

Table 3: Measured and accepted energy spacings between the ^{87}Rb F=1 ground state to first excited state transitions. Accepted values [9,10]

For the ^{87}Rb F=1 spectrum, there was likely a slight systematic error in recorded data. All three measurements were higher than the accepted values by a similar amount, about 7 or 9 MHz. The data in Figure 20 shows a systematic slope under the peaks. This likely resulted from relative differences between each of the photodiode's outputs as a function of the scanned laser, which changed the absorption profiles that were subtracted by the

difference amplifier. The photodiodes could have registered different signals from small changes in alignment of lasers as it was scanned. The added slope tends to shift the peaks to higher frequencies, which might result in being systematically higher than accepted values.

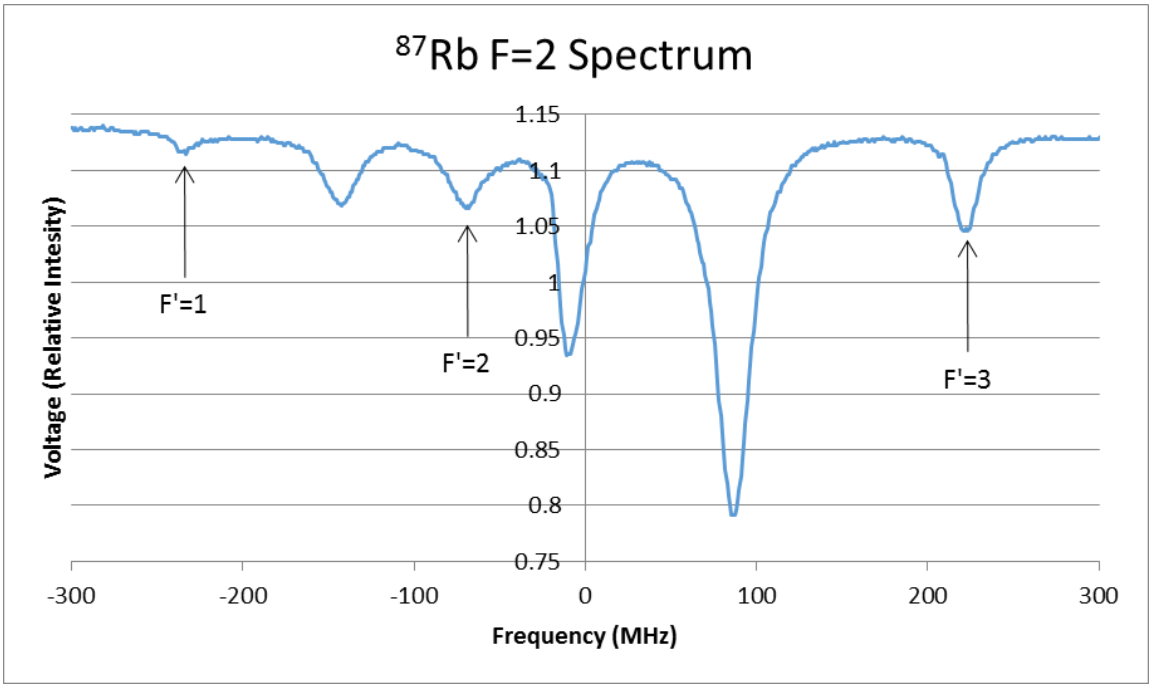

Figure 21: Spectrum of hyperfine energy splittings from the ^{87}Rb F=2 ground state to first excited state transitions.

87Rb F=2 Spectrum		
Frequency Spacing (MHz)		**Accepted Values**
F'=1 & 2	167 ± 11MHz	156.947 ± 0.007MHz
F'=2 & 3	291 ± 6MHz	266.650 ± 0.009MHz
F'=1 & 3	458 ± 10MHz	423.597 ± 0.011 MHz

Table 4: Measured and accepted energy spacings between the ^{87}Rb F=2 ground state to first excited state transitions. Accepted values [9,10]

Final measurements for the ^{87}Rb F=2 energy splittings also appear to be consistently larger than the accepted values, but not for the same reason as the ^{87}Rb F=1 spectrum. The data shows no signs of a systematic slope up-shifting peaks and the peaks are narrow and measurable within a reasonable uncertainty. However this inconsistency with accepted values could possibly derive from factors such as small changes in the voltage ramp scanning the laser during collection. In principle the data could be remeasured to test this hypothesis.

5.0 Discussion

The Fabry-Pérot Interferometer data was used to calibrate the spectra into units of frequency due to its overall smaller relative uncertainty than the Michelson Interferometer. For both of these interferometers, relative uncertainty derived from the width of output peaks, and therefore the uncertainty with which the peak could be located, as well as the uncertainties of the Δf between successive peaks (Equations 10 and 16). The manufacturer gave a 0.5% uncertainty on the radius of the mirrors (related to length of the cavity L) for the Fabry-Pérot interferometer. This calibration data contributed to the uncertainty of measurements of energy spacings in the spectra. Uncertainty on these final spacing measurements also derived from the width of the peaks in the spectra; again the width of these peaks yielded an uncertainty to which the location of the peak was actually known. When the energy levels were relatively close together, the Lamb dips in the output began to run together, smoothing out the curve and decreasing the certainty of peak locations; this effect was particularly observable in the case of the ^{85}Rb F=2 transitions (Figure 18) with 10.1% deviation from accepted energy spacings. The ^{87}Rb F=1 spectrum however, with its systematic error, accounted for the

largest deviation from accepted energy spacings, including a maximum 12.2% error. Other spectra measurements were in better agreement, possessing smaller error (ranging between 2.1% and 10.1%) than this and some agreeing with accepted measurements to within uncertainty. The measurements that were conducted were measured to a few MHz and the results aligned reasonably with current accepted values.

Final data could have been improved through changing interferometers' geometric properties; increasing the difference in path length ΔL for the Michelson and the length of the cavity L for the Fabry-Pérot would have decreased the uncertainty of their calibration data. Also by further enlarging the geometry of the saturated absorption setup (Figure 11) the pump beam could have been aligned at a smaller angle from antiparallel with the probe beam. The closer the pump beam was to completely overlapping the probe beam, the more effectively it could have saturated excitations, thus leaving sharper, more defined lamb dips for the spectra.

It is important to recognize that this final data is only the energy splittings of the first excited state, not the absolute frequencies of transitions from ground to excited state. This is a result of the tremendous difference of scale of the measurement and the small range over which the laser is scanned. The laser is scanned over such a small range of frequencies, (over energy splittings with $\Delta f \geq 30\ MHz$) compared to the much larger absolute transition of about $3 \cdot 10^8\ MHz$. This would be like measuring the height of 723 Mt. Everests to within the precision of the diameter of a golf ball. While this technique and laser allowed for very precise, small measurements of the energy splittings, it does not allow us to measure the full transition energy from ground to excited states.

References

[1]M. Saffman and T.G. Walker, *Quantum information with Rydberg atoms*, Vol 3, Issue 3. (American Physical Society, 2010) pp. 2313-2363.

[2]E. Hecht and A. Zajac, *Optics*, 1st Ed. (Addison-Wesley Publishing Co, Reading, MA, 1974) pp. 481-483.

[3]D. O'Shea, W.R. Callen, W.T. Rhodes, *Introduction to Lasers and Their Applications*, (Addison-Wesley Publishing Co, Reading, MA, 1978).

[4]M.C. Schu, *External Caivity Diode Lasers: Controlling Laser Output via Optical Feedback*, (College of William and Mary, Williamsburg, VA, 2003), pp. 6-17.

[5]R.S. Conroy *et al.*, *A Visible Extended Cavity Diode Laser for the Undergraduate Laboratory*, American Journal of Physics 68 (10), (2000).

[6]C. Palmer and E. Loewen, *Diffraction Grating Handbook*, 6th Ed. (Newport Corporation, Rochester, NY, 2005).

[7]D. A. Steck, *Rubidium 85 D Line Data*, http://steck.us/alkalidata (revision 2.1.6, 20 September 2013).

[8]E. Arimondo, M. Inguscio, and P. Violino, *Experimental determinations of the hyperfine structure in the alkali atoms*, Reviews of Modern Physics 49, 31 (1977).

[9]A. Banerjee, D. Das, and V. Natarajan, *Absolute frequency measurements of the D1 lines in ^{39}K, ^{85}Rb, and ^{87}Rb with ~ 0.1 ppb uncertainty*, Europhysics Letters 65, 172 (2004).

[10]G. P. Barwood, P. Gill, andW. R. C. Rowley, *Frequency Measurements on Optically Narrowed Rb-Stabilised Laser Diodes at 780 nm and 795 nm*, Applied Physics B 53, 142 (1991).

Appendices

A1: Personally constructed external cavity diode laser. Includes metal housing, diode, adjustable mount, electronic drivers, diffraction grating, temperature regulator, and PZT

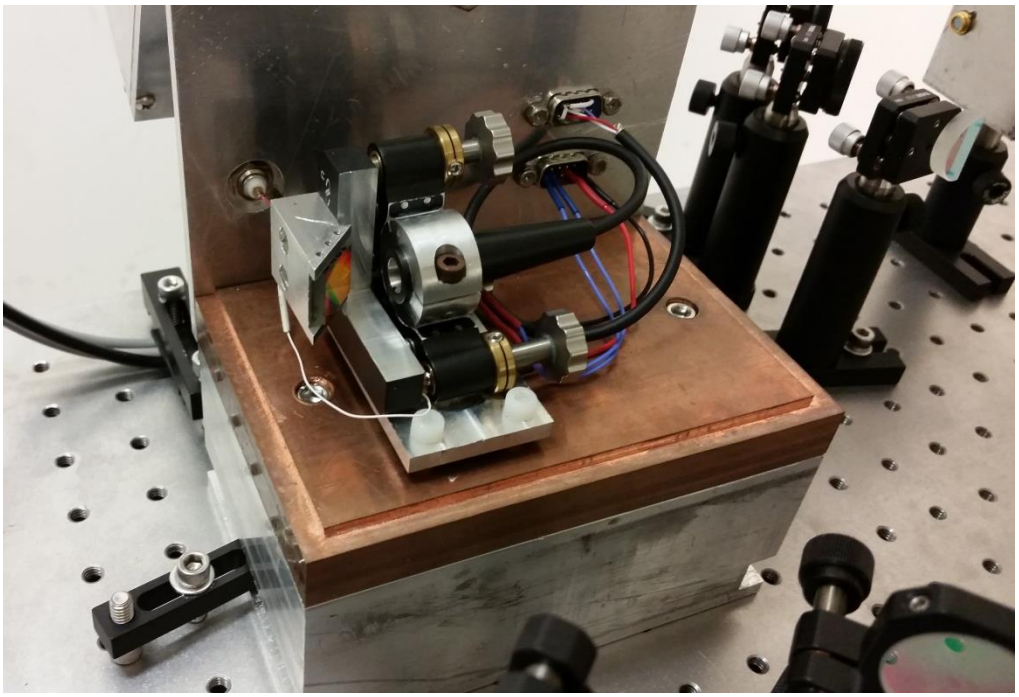

A2: Saturated absorption spectroscopy setup in Otterbein University lab